All-boron fullerene B_{40}: a superatomic structure

Jia Wang[1,2†], Tianrong Yu[1,2†], Yang Gao[1,2] and Zhigang Wang[1,2*]

ABSTRACT By means of the first-principles calculations, we reveal that B_{40} presents superatomic properties. It not only has superatomic 1S, 1P, 1D and 1F orbitals, but also has superatomic orbitals 2S, 2P, 2D and 2F. The superatomic 2F orbital of B_{40} is partially occupied, thus adding six electrons to the cluster leads to a superatomic structure of fully occupied shells. The computed nucleus-independent chemical shift values suggest that the B_{40}^{6-} is of higher electron delocalization than B_{40} itself. Our work opens up a new perspective for the superatomic physics in boron fullerene family.

Keywords: boron fullerene, superatom, electronic structure, first-principles

The all-boron fullerene B_{40}, discovered in 2014, has greatly enriched the chemistry of boron and may lead to the development of new boron-based nanomaterials [1]. Subsequently, the stabilities and electronic properties of endohedral metal complexes of B_{40} have also been investigated [2–4]. Among the clusters with various sizes, those deemed "superatoms" exhibit enhanced stabilities due to the electronic shell closing [5]. Many superatomic structures, such as C_{60} [6], Al_{13} [7], Na_{40} [8] and Au_{20} [9], have been experimentally confirmed. Recently, the Au_{32} gold fullerene was revealed to have $1S^21P^61D^{10}1F^{14}$ electronic configuration, thus making a superatom [10,11]. Similarly, as a hollow cage structure, is B_{40} fullerene also a superatom? Answering this question is crucial for us to understand the stabilities of B_{40} and its derivatives, and explore their potential applications.

In this work, by means of density functional theory (DFT) computations [12], we carefully analyzed the nature of electronic structure of the all-boron fullerene B_{40}. Our calculations reveal that the neutral B_{40} fullerene is a superatom with partially occupied 2F shell. However, by adding six electrons or removing eight electrons, a superatom can be formed with fully occupied shells. In addition, B_{40}^{6-} and B_{40}^{8+} with fully occupied shells are

highly aromatic as indicated by the negative nucleus-independent chemical shift (NICS) values at the cage center.

The geometric structure of B_{40} was fully optimized using generalized gradient approximation (GGA) functional Perdew-Burke-Ernzerhof (PBE) [13] and hybrid functionals PBE0 [14], B3LYP [15,16] and HSE06 [17,18] with 6-31G* basis sets [19], and the relative energies between different electronic states were listed in Table S1 in Supplementary information(SI). The charged species of B_{40}, namely, B_{40}^{6-} and B_{40}^{8+}, were also optimized at PBE0/6-31G* level. Frequency analyses were performed at the same level of theory to characterize the nature of the stationary points. Both B_{40} and B_{40}^{6-} are true local minima, but B_{40}^{8+} with fully occupied shell is a high order saddle point. Following the imaginary modes of B_{40}^{8+} leads to the true local minimum without full-filled shell. The optimized geometries from different functionals are rather similar, and we only discuss the computational results from PBE0 because it has been tested extensively in previous works and found to be suitable for boron clusters [1,20–22]. To investigate the electron delocalization or aromaticity of B_{40} and its charged species, we calculated NICS (in ppm) [23,24] at the cage centers of the optimized geometries of the empty cage molecules using the gauge-independent atomic orbital (GIAO) method [25]. The verification of B_{40} using PBE0/6-311 +G* level is shown in Table S2 in SI. All computations are carried out using the Gaussian09 package [26].

Our calculations show that the ground state of B_{40} fullerene (D_{2d}) is non-spin-polarized singlet, with the low and high energy molecular orbitals (MOs) displayed in Figs 1, 2, respectively. Among the low-energy MOs, a double-occupied MO $7a_1$ (marked by black) resembles an s-like atomic orbital, thus we call it the 1S superatomic orbital (that is, molecular orbital) for B_{40}, and the specific orbital composition analyses are described in the fol-

[1] Institute of Atomic and Molecular Physics, Jilin University, Changchun 130012, China
[2] Jilin Provincial Key Laboratory of Applied Atomic and Molecular Spectroscopy (Jilin University), Changchun 130012, China
† These authors contributed equally to this paper.
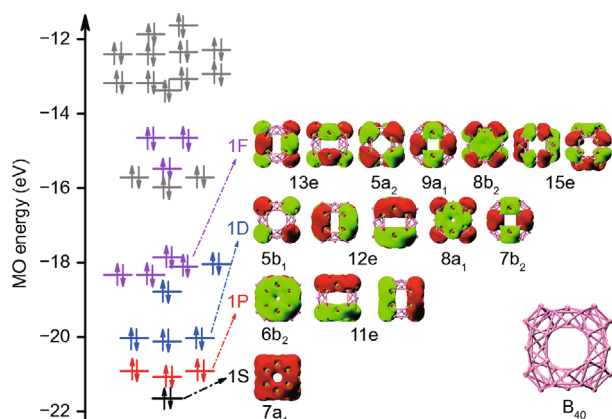* Corresponding author (emails: wangzg1978@hotmail.com or wangzg@jlu.edu.cn)

Figure 1 Low-energy MOs of B_{40} fullerene at the PBE0 level of theory. 1S, 1P, 1D and 1F represent superatomic MOs of B_{40} fullerene. The MOs marked by black, red, blue and pink represent the 1S, 1P, 1D and 1F superatomic orbitals, respectively, while other MOs are given in gray. The MOs lower than $7a_1$ are contributed to 1s atomic orbitals of boron atoms and are not given.
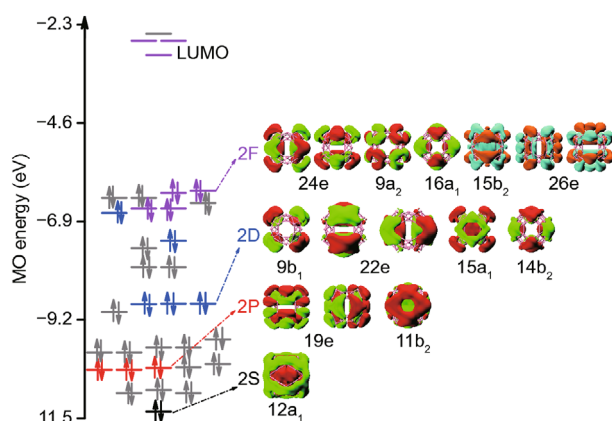

Figure 2 High-energy MOs of B_{40} fullerene at the PBE0 level of theory. 2S, 2P, 2D and 2F represent superatomic MOs of B_{40} fullerene, respectively. The superatomic MOs indicated by green and red are double-occupied MOs, while those indicated by orange and blue are unoccupied MOs.

lowing. This 1S orbital is followed by three p-like atomic orbitals, namely, the $6b_2$ and 11e MOs (denoted by red), which are actually the 1P superatomic orbitals of B_{40}. Then, there are five d-like orbitals, namely, $5b_1$, 12e, $8a_1$ and $7b_2$ (marked by blue), which are the 1D superatomic orbitals for B_{40} fullerene. What follows are the seven f-like orbitals, 13e, $5a_2$, $9a_1$, $8b_2$ and 15e (marked by pink), which are essentially the 1F superatomic orbitals of B_{40} fullerene. The symmetry and energy level diagram of these orbitals clearly show the 1S, 1P, 1D and 1F electronic shells of the B_{40} cage.

The MOs at higher energy levels are much more complex. With increasing energy levels, the MOs were

characterized with higher angular momentum (Fig. 2). For example, the MO $12a_1$ is s-like, and is called superatomic orbital 2S. Similarly, we can easily recognize three 2P superatomic orbitals (19e and $11b_2$) and five 2D superatomic orbitals ($9b_1$, 22e, $15a_1$ and $14b_2$). However, the 2F superatomic orbitals split into two sets, the four double-occupied MOs (24e, $9a_2$ and $16a_1$) and the three unoccupied MOs ($15b_2$ and 26e), with a substantial gap. The large splitting reflects the breaking of spherical symmetry, hence there is a hiatus in the spherical levels [27]. Compared to the 1S, 1P, 1D, 1F superatomic orbitals, the MOs energies of 2S, 2P, 2D and 2F are more dispersed, because some high angular momentum superatomic orbitals 1G, 1H, 1I (see Fig. S1) and other σ bond orbitals are inserted among these energy levels. Combined with previous research of chemical bonding in all-boron fullerenes [1], we summarized superatomic configurations for $1(S^{\sigma})^2 1(P^{\sigma})^6 1(D^{\sigma})^{10} 1(F^{\sigma})^{14}$ and $2(S^{\pi})^2$ $2(P^{\pi})^6 2(D^{\pi})^{10} 2(F^{\pi})^8$. Superatomic orbitals 1G, 1H and 1I are also constituted by σ bond. Moreover, unlike the C_{60}, the B_{40} is an electron-deficient structure, which may be because it is not a complete sphere, so there are 16 σ bond orbitals that cannot be clearly classified as superatomic orbitals. Recently, the report of $U@B_{40}$ indicates that the 2S, 2P, 2D and 2F of B_{40} are respectively bonding with U-7s, U-7p, U-6d and U-5f to form a closed-shell superatomic structure [28]. Considering symmetric combination of orbitals, this further proves that although superatomic shells 2F are not fully filled, they can also be classified according to the atomic orbitals, highlighting the B_{40} has a superatom feature. In addition, similar to previous research that $[U@C_{28}]^{2+}$ [29], $U@C_{28}$ [30], $U@Au_{14}$ [31], $Th@Ag_{14}$ [32] are superatom, their outer spherical clusters are also superatoms.

Furthermore, we analyzed the composition of these superatomic orbitals for B_{40} fullerene (Fig. 3). For the superatomic orbitals 1S, the contribution of 2s atomic orbitals of boron atoms in B_{40} fullerene is 84.99%, and that of 2p is 10.32%. Three 1P superatomic orbitals mainly originate from the contributions of 2s shell of boron atoms, with contributions from 82% to 85% for 2s and from 9% to 12% for 2p. For five 1D and seven 1F superatomic orbitals, the 2s contributions are 59%–79% and 41%–63%, while the 2p contributions are 18%~35% and 34%~54%, respectively. In contrast, the 2S, 2P, 2D and 2F superatomic orbitals are primarily derived from the 2p contributions. In summary, the contribution from boron atoms' 2s orbitals in B_{40} fullerene gradually decreases, while that from 2p gradually increases from 1S to 1F. Furthermore, the superatomic orbitals that "principal
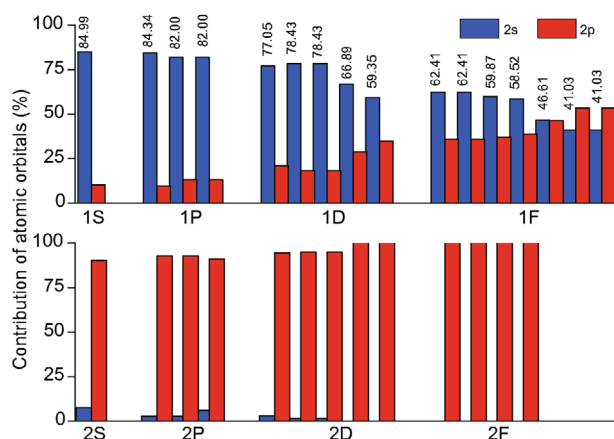
Figure 3 Contribution of superatomic orbitals for B_{40} fullerene. Blue represents the contribution of 2s atomic orbitals and red denotes the contribution of 2p atomic orbitals. The values in figure are the contribution percentage for 2s.

quantum number" is 2 mainly originate from the 2p atomic orbitals of boron atoms in B_{40} fullerene.

In order to further demonstrate that B_{40} fullerene is a superatomic structure, we added or removed electrons from the neutral B_{40} fullerene to form the full-shell electronic structure. As shown in Fig. 2, the lowest unoccupied molecular orbital (LUMO), LUMO+1 and LUMO+2 of B_{40} are three unoccupied 2F superatomic orbitals, thus we added six electrons to the neutral B_{40} to form B_{40}^{6-}. As expected, our computations show that B_{40}^{6-} is a closed-shell singlet state, and of a fully occupied electronic shells (Fig. 4; the other superatomic orbitals of B_{40}^{6-} are provided in Fig. S2). Moreover, the 2F shell of the neutral B_{40} is only occupied by eight electrons, and removing this eight electrons leads to B_{40}^{8+}. We can also obtain a closed-shell singlet state and its superatomic shells are fully occupied, as shown in Figs S3, S4. However, note that this B_{40}^{8+} with full shell is not a local minimum, and the superatomic shell of the true local minimum for B_{40}^{8+} is not full-filled shown in Figs S5, S6.

Aromaticity plays an important role in determining the stability of a spherical cluster [33,34]. To probe the electron delocalization of neutral and charged B_{40} species, we calculated the NICS values at their cage centers. The NICS value calculated at the GIAO-PBE0/6-311+G* level of theory for neutral B_{40} is −41.8 ppm and for B_{40}^{6-} is −63.4 ppm. And the value for B_{40}^{8+} with fully occupied electronic shells is −71.0 ppm (shown in Table S2), while that for ground state of B_{40}^{8+} is 4.1 ppm. Thus, the neutral B_{40}, B_{40}^{6-} and full-shell B_{40}^{8+} are aromatic, especially B_{40}^{6-} and B_{40}^{8+} with fully occupied shells are highly aromatic.
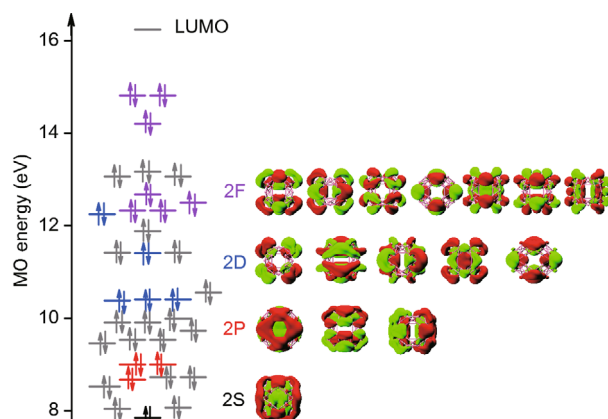

Figure 4 Higher MOs energy diagrams for the ground state of B_{40}^{6-} at PBE0.

Interestingly, the true local minimum of B_{40}^{8+} is non-aromatic, which suggests that aromaticity determines the stability of the electronic structure and it is not the sole factor for cluster stability.

We investigated the electronic structure of B_{40} fullerene using first-principles methods with different pure and hybrid functionals. Our results clearly show that B_{40} fullerene possesses superatomic properties and its electronic configuration contains $1S^2 1P^6 1D^{10} 1F^{14}$ which mainly originate from 2s atomic orbitals of boron atoms. B_{40} fullerene also contains more complex high angular momentum superatomic orbitals 2S, 2P, 2D and 2F, whose orbital compositions are primarily contributed by 2p shell. Research of B_{40}^{6-} shows that adding six electrons to B_{40} fullerene can form a stable full shell superatomic structure. The NICS values show that the closed-shell superatomic structures B_{40}^{6-} and B_{40}^{8+} have higher aromaticity and electron delocalization than neutral B_{40}.

It is well known that the valence electrons of carbon fullerene are sp^2 hybridized, such as C_{60}, and similarly, the valence electrons of boron are also sp^2 hybridized [35]. It is particularly important that, after C_{60}, B_{40} is the second non-metallic cage molecule discovered by experiment. Moreover, the C_{60} superatomic orbitals are contributed to the p_z electrons of carbon atom [6,36], which can be used scalar harmonics [37]. Unlike C_{60}, boron forms cluster bonds by both s and p orbitals, which requires the use of

Table 1 NICS (in ppm) at the cage centers of B_{40} and its ions computed at the GIAO-PBE/6-311+G* and GIAO-PBE0/6-311+G* levels of theory based on the PBE0/6-31G* structures

Charge	−6	0	+8
NICS (PBE0)	−63.4	−41.8	4.1
NICS (PBE)	−72.3	−39.3	33.4

tensor surface harmonics [38,39]. Analogous to C_{60}, B_{40} is widely used in metalloborospherenes [2,40] or as hydrogen storage materials [41]. Furthermore, as superatom, because B_{40} is highly robust and dynamically stable at high temperatures [1], so it may bring outburst of density of states and has potential applications in high-temperature superconductivity [42].

1   Zhai HJ, Zhao YF, Li WL, et al. Observation of an all-boron fullerene. Nat Chem, 2014, 447: 727–731

2   Jin P, Hou Q, Tang C, et al. Computational investigation on the endohedral borofullerenes M@B_{40} (M = Sc, Y, La). Theor Chem Acc, 2015, 134: 13

3   Fa W, Chen S, Pande S, et al. Stability of metal-encapsulating boron fullerene B_{40}. J Phys Chem A, 2015, 119: 11208–11214

4   Li Y. Perfectly planar CoB_{18}–as a motif for metallo-borophenes. Nano Res, 2016, 9: 1877–1878

5   de Heer WA. The physics of simple metal clusters: experimental aspects and simple models. Rev Mod Phys, 1993, 65: 611–676

6   Feng M, Zhao J, Petek H. Atomlike, hollow-core-bound molecular orbitals of C_{60}. Science, 2008, 320: 359–362

7   Leuchtner RE, Harms AC, Castleman Jr. AW. Thermal metal cluster anion reactions: behavior of aluminum clusters with oxygen. J Chem Phys, 1989, 91: 2753–2754

8   Knight WD, Clemenger K, de Heer WA, et al. Electronic shell structure and abundances of sodium clusters. Phys Rev Lett, 1984, 53: 510–510

9   Li J, Li X, Zhai HJ, et al. Au_{20}: a tetrahedral cluster. Science, 2003, 299: 864–867

10 De HS, Krishnamurty S, Pal S. A first principle investigation on the thermal stability of a golden fullerene: a case study of Au_{32}. Catal Today, 2012, 198: 106–109

11 Johansson MP, Sundholm D, Vaara J. Au_{32}: a 24-carat golden fullerene. Angew Chem Int Ed, 2004, 43: 2678–2681

12 Parr RG. Density functional theory. Annu Rev Phys Chem, 1983, 34: 631–656

13 Perdew JP, Burke K, Ernzerhof M. Generalized gradient approximation made simple. Phys Rev Lett, 1996, 77: 3865–3868

14 Adamo C, Barone V. Toward reliable density functional methods without adjustable parameters: the PBE0 model. J Chem Phys, 1999, 110: 6158–6170

15 Lee C, Yang W, Parr RG. Development of the Colle-Salvetti correlation-energy formula into a functional of the electron density. Phys Rev B, 1988, 37: 785–789

16 Miehlich B, Savin A, Stoll H, et al. Results obtained with the correlation energy density functionals of becke and Lee, Yang and Parr. Chem Phys Lett, 1989, 157: 200–206

17 Heyd J, Scuseria GE, Ernzerhof M. Hybrid functionals based on a screened Coulomb potential. J Chem Phys, 2003, 118: 8207–8215

18 Krukau AV, Vydrov OA, Izmaylov AF, et al. Influence of the exchange screening parameter on the performance of screened hybrid functionals. J Chem Phys, 2006, 125: 224106–224106

19 Hehre WJ, Ditchfield R, Pople JA. Self-consistent molecular orbital methods. XII. Further extensions of Gaussian—type basis sets for use in molecular orbital studies of organic molecules. J Chem Phys, 1972, 56: 2257–2261

20 He R, Zeng XC. Electronic structures and electronic spectra of all-boron fullerene B_{40}. Chem Commun, 2015, 51: 3185–3188

21 Piazza ZA, Hu HS, Li WL, et al. Planar hexagonal B_{36} as a potential basis for extended single-atom layer boron sheets. Nat Commun, 2014, 5: 3113

22 Kiran B, Bulusu S, Zhai HJ, et al. Planar-to-tubular structural transition in boron clusters: B_{20} as the embryo of single-walled boron nanotubes. Proc Natl Acad Sci USA, 2005, 102: 961–964

23 Schleyer PR, Maerker C, Dransfeld A, et al. Nucleus-independent chemical shifts: a simple and efficient aromaticity probe. J Am Chem Soc, 1996, 118: 6317–6318

24 Chen Z, Wannere CS, Corminboeuf C, et al. Nucleus-independent chemical shifts (NICS) as an aromaticity criterion. Chem Rev, 2005, 105: 3842–3888

25 Wolinski K, Hinton JF, Pulay P. Efficient implementation of the gauge-independent atomic orbital method for NMR chemical shift calculations. J Am Chem Soc, 1990, 112: 8251–8260

26 M. J. Frisch, G. W. Trucks, H. B. Schlegel, et al. Gaussian 09, revision d.01. , 2013

27 Ceulemans A, Compernolle S, Lijnen E. Hiatus in the spherical shell model of fullerenes. Phys Chem Chem Phys, 2004, 6: 238–241

28 Yu T, Gao Y, Xu D, et al. Actinide endohedral boron clusters: a closed-shell electronic structure of U@B_{40}. Nano Res, 2017, doi: 10.1007/s12274-017-1637-9

29 Dognon JP, Clavaguera C, Pyykko P. A predicted organometallic series following a 32-electron principle: An@C_{28}(An = Th, Pa^+, U^{2+}, Pu^{4+}). J Am Chem Soc, 2009, 131: 238–243

30 Dai X, Gao Y, Jiang W, et al. U@C_{28} : the electronic structure induced by the 32-electron principle. Phys Chem Chem Phys, 2015, 17: 23308–23311

31 Gao Y, Wang Z. Effects of 5f-elements on electronic structures and spectroscopic properties of gold superatom model. Chin Phys B, 2016, 25: 083102

32 Gao Y, Jiang W, Chen L, et al. First-principles study on charge transfer in an actinide-containing superatom from surface-enhanced Raman scattering. J Mater Chem C, 2017, 5: 803–806

33 Chen Z, Neukermans S, Wang X, et al. To achieve stable spherical clusters: general principles and experimental confirmations. J Am Chem Soc, 2006, 128: 12829–12834

34 Xu C, Cheng L, Yang J. Double aromaticity in transition metal centered double-ring boron clusters M@B_{2n}(M = Ti, Cr, Fe, Ni, Zn; n = 6, 7, 8). J Chem Phys, 2014, 141: 124301

35 Gonzalez Szwacki N, Sadrzadeh A, Yakobson BI. B_{80} fullerene: an ab initio prediction of geometry, stability, and electronic structure. Phys Rev Lett, 2007, 98: 166804

36 Zhang GP, Zhu HP, Bai YH, et al. Imaging superatomic molecular orbitals in a C_{60} molecule through four 800-nm photons. Int J Mod Phys B, 2015, 29: 1550115

37 Troullier N, Martins JL. Structural and electronic properties of C_{60}. Phys Rev B, 1992, 46: 1754–1765

38 Zhang Q. Notes on the tensor surface harmonic method. J Mol Structure-Theochem, 1984, 109: 215–221

39 Stone AJ, Wales DJ. A new structural tensor surface harmonic bonding theory. Mol Phys, 1987, 61: 747–765

40 Bai H, Chen Q, Zhai HJ, et al. Endohedral and exohedral metalloborospherenes: M@B_{40}(M=Ca, Sr) and B_{40} (M=Be, Mg). Angew Chem Int Ed, 2015, 54: 941–945

41 Dong H, Hou T, Lee ST, et al. New Ti-decorated B_{40} fullerene as a promising hydrogen storage material. Sci Rep, 2015, 5: 9952

42 Halder A, Liang A, Kresin VV. A novel feature in aluminum

cluster photoionization spectra and possibility of electron pairing at $T \gtrsim 100$ K. Nano Lett, 2015, 15: 1410–1413

Author contributions Wang J and Yu T contributed equally to this work. Wang Z proposed the project; Wang J calculated and analyzed the results. All authors contributed to the general discussion.

Conflict of interest The authors declare that they have no conflict of interest.

Supplementary information Superatomic orbitals energy diagrams are available in the online version of the paper.

Jia Wang was born in 1990. Currently, she is a PhD candidate in Prof. Zhigang Wang's group at the Institute of Atomic and Molecular Physics, Jilin University. Her current research direction is the spin polarization effect of p electrons.

Zhigang Wang received his BSc degree from the College of Physics, Jilin University in 2001 and his PhD degree from the Institute of Atomic and Molecular Physics, Jilin University in 2006, under the supervision of Prof. Shoufu Pan. He joined the Institute of Atomic and Molecular Physics, Jilin University in 2011 as a full professor. His research interests are focused on the interactions in complex molecular systems.

全硼富勒烯B$_{40}$：一个超原子结构

王佳[1,2†]，于天荣[1,2†]，高阳[1,2]，王志刚[1,2*]

摘要 本文利用第一性原理计算，发现B$_{40}$表现出超原子特性，不仅有1S, 1P, 1D, 1F超原子轨道，还有2S, 2P, 2D 和2F超原子轨道. 由于B$_{40}$的2F壳层是部分占据，因此添加6个电子到B$_{40}$上将导致一个满占据壳层的超原子结构. 核独立化学位移的计算结果显示B$_{40}^{6-}$的电子离域性比B$_{40}$高. 本工作开创了一个硼富勒烯家族中超原子物理新视角.